

Supporting Information

Ultrapure Green Light Emission in One-dimensional Hybrid Lead Perovskite: Achieving Recommendation 2020 Standard

Chang-Qing Jing,^{a,b} Qi-Long Liu,^a Cheng-Hao Zhao,^a Yan-Yu Zhao,^a Cheng-Yang Yue,^{a,b*} and
Xiao-Wu Lei^{a,b*}

^aCollege of Chemistry, Chemical Engineering and Materials, Jining University, Qufu, Shandong,
273155, P. R. China

^bCollege of Chemistry and Chemical Engineering, Qufu Normal University, Qufu, Shandong,
273165, P. R. China

Experimental Section

Figure S1. The coordination environments of Pb1 (a) and Pb2 (b) atoms, schematic of 1D $[\text{Pb}_3\text{Br}_{10}]^{4-}$ chain (c) and the packing framework along the *c*-axis (d) of compound $[\text{TMPDA}]_2\text{Pb}_3\text{Br}_{10}$.

Figure S2. The PXRD patterns of bulk and microscale crystals of $[\text{TMPDA}]_2\text{Pb}_3\text{Br}_{10}$ as well as simulated data from single crystal structure.

Figure S3. The XPS spectra of Pb, Br, C and N atoms in $[\text{TMPDA}]_2\text{Pb}_3\text{Br}_{10}$.

Figure S4. The IR spectrum of compound $[\text{TMPDA}]_2\text{Pb}_3\text{Br}_{10}$.

Figure S5. The SEM photos (a and c) and corresponding EDX spectrum (b and d) as well as the contents of lead and bromine elements (e and f) for bulk crystals of $[\text{TMPDA}]_2\text{Pb}_3\text{Br}_{10}$.

Figure S6. The SEM photos of single crystals (a) and EDX elemental mapping images of Pb and Br elements of $[\text{TMPDA}]_2\text{Pb}_3\text{Br}_{10}$.

Figure S7. (a) The solid-state UV-Vis absorption spectrum of $[\text{TMPDA}]_2\text{Pb}_3\text{Br}_{10}$, (b) the Tauc plots based on the assumptions of direct and indirect transitions.

Figure S8. The calculated electronic band structure (a), total and partial density of states (b), charge density of lowest unoccupied molecular orbital (c) and highest occupied molecular orbital (d) for $[\text{TMPDA}]_2\text{Pb}_3\text{Br}_{10}$.

Figure S9. The PLQY of bulk crystals for compound $[\text{TMPDA}]_2\text{Pb}_3\text{Br}_{10}$.

Figure S10. The time-resolved PL decay curve of $[\text{TMPDA}]_2\text{Pb}_3\text{Br}_{10}$ bulk crystals at 100 K.

Figure S11. The SEM photos of microscale crystals (a) and bulk crystals (b) of $[\text{TMPDA}]_2\text{Pb}_3\text{Br}_{10}$.

Figure S12. The thermogravimetric analysis curve for $[\text{TMPDA}]_2\text{Pb}_3\text{Br}_{10}$.

Figure S13. The thermogravimetric analysis curve for $[\text{TMPDA}]_2\text{Pb}_3\text{Br}_{10}$.

Figure S14. Comparison of the PXRD patterns of $[\text{TMPDA}]_2\text{Pb}_3\text{Br}_{10}$ before and after heating at various temperature from 50 °C to 200 °C.

Figure S15. Comparison of the normalized PL emission spectra of $[\text{TMPDA}]_2\text{Pb}_3\text{Br}_{10}$ before and after heating from 50 °C to 200 °C.

Figure S16. The PXRD patterns of $[\text{TMPDA}]_2\text{Pb}_3\text{Br}_{10}$ before and after storing in humid air (> 90%) or exposure under UV light irradiation.

Figure S17. Comparison of the normalized PL emission spectra of [TMPDA]₂Pb₃Br₁₀ before and after exposure in humid air for one year at room temperature.

Figure S18. Comparison of the normalized PL emission spectra of [TMPDA]₂Pb₃Br₁₀ before and after exposure in UV light irradiation for 48 hours at 300 K.

Figure S19. The XPS spectra of Pb, Br, C and N atoms for [TMPDA]₂Pb₃Br₁₀ after long-term exposure under strong UV-light irradiation.

Figure S20. The PXRD patterns of [TMPDA]₂Pb₃Br₁₀ after soaking in various organic solvents for one day.

Figure S21. The PL emission spectra of [TMPDA]₂Pb₃Br₁₀ before and after soaking in various organic solvents for one day.

Figure S22. The experimental powder X-ray diffraction data of prepared [TMPDA]₂Pb₃Br₁₀ based film and simulated data.

Figure S23. The PL emission spectrum of prepared [TMPDA]₂Pb₃Br₁₀ based film at 300 K.

Figure S24. Anti-counterfeiting application of [TMPDA]₂Pb₃Br₁₀: the photo images of printed patterns on commercial parchment paper under ambient light (a) and a 365 nm UV lamp (b).

Table S1. Summary of the green light emissions of representative commercial inorganic green phosphors.

Table S2. Summary of the green light emissions of representative commercial inorganic green phosphors.

Table S3. The comparison of calculated Huang-Rhys factors for various luminescent materials.

Table S4. Comparison of color gamut in CIE 1931 color space of fabricated WLED based on green light emitting phosphors.

Table S5. Crystal Data and Structural Refinements for compound [TMPDA]₂Pb₃Br₁₀.

Table S6. Selected bond lengths (Å) and bond angles (°) for compound [TMPDA]₂Pb₃Br₁₀.

Table S7. Hydrogen bonds data for compound [TMPDA]₂Pb₃Br₁₀.

Experimental Section

Chemical Materials: All the following purchased precursor materials were directly used without any physical purification: PbBr_2 (99.9%), tetramethyl-1,3-diaminopropane (TMPDA, 99.0%), N-methylformamide (NMF, 99.5%), ethanol (EtOH, 99.0%), acetone (99.0%), acetonitrile (MeCN, 99.0%), methanol (99.0%) and hydrobromic acid (HBr , $\geq 40.0\%$).

Synthesis of $[\text{TMPDA}]_2\text{Pb}_3\text{Br}_{10}$: The mixture of PbBr_2 (0.110 g, 0.3 mmol) and TMPDA (0.100 g, 0.5 mmol) was dissolved in a mixed solution of NMF (4 mL), EtOH (2 mL) and hydrobromic acid (1 mL). The suspension was constantly stirred about half an hour and then transfer into a 25 mL glass vial, which was then sealed and heated at constant temperature of 100 °C at seven days. After the reaction, it was cooled to room temperature at a rate of 10 °/h, and lots of light-green plane-like crystals were filtrated from the vial and washed with ethanol three times (yield: 88% base on Pb). The structure was subsequently determined to be $\text{C}_{14}\text{H}_{40}\text{N}_4\text{Pb}_3\text{Br}_{10}$ by using the single crystal X-ray diffraction. Elemental analysis calculated for $\text{C}_{14}\text{H}_{40}\text{N}_4\text{Pb}_3\text{Br}_{10}$: C, 9.97 %; N, 3.32 %; H, 2.30 %; found: C, 9.85 %; N, 3.24 %; H, 2.36 %. IR (KBr, cm^{-1}): 3440(*m*), 3190(*w*), 2740(*w*), 1630 (*s*), 1400(*s*) and 940 (*w*).

Characterizations: The powder X-ray diffraction experiments were performed on a Bruker D8 Advance X-ray powder diffraction meter operating at 40 kV and 40 mA (Cu- $\text{K}\alpha$ radiation, $\lambda = 1.5418 \text{ \AA}$). The diffraction pattern was scanned over the angular range of 5-60 degree with a step size of 0.02 at room temperature. The solid state UV-Vis optical absorption spectrum for powder sample was collected at PE Lambda 900 UV/Vis spectrophotometer at room temperature in wavelength range of 200-800 nm. The bandgap is determined by fitting the absorption spectrum using Tauc function. The FT-IR spectra were measured as KBr pellets on a Nicolet Magna 750 FT-IR spectrometer in the range of 4000-400 cm^{-1} . The thermogravimetric analysis (TGA) was carried out on a Mettler TGA/SDTA 851 thermal analyzer from room temperature to 800 °C under the flow of nitrogen atmosphere. The XPS spectra were tested on the Escalab XI + instrument, USA. SEM and DEX images were performed in Hitachi SU-8010 field emission scanning electron microscopy.

Single-crystal X-ray diffraction: A Bruker Apex II CCD diffractometer with Mo $\text{K}\alpha$ radiation ($\lambda = 0.71073 \text{ \AA}$) was utilized for single crystal X-ray diffraction and the measurement was performed at 293 K. The *APEX3* software was used for data reduction and multi-scans absorption correction.

SHELXLTL software was applied to solve crystal structure using direct methods. And the structure was refined by the full matrix method based on F^2 using the package SHELXS-97.²⁸ All the non-hydrogen atoms were refined with anisotropic thermal parameters, and hydrogen atoms of organic molecules were positioned geometrically and refined isotropically. Structural refinement parameters of [TMPDA]₂Pb₃Br₁₀ are summarized in Table S5 and important bond lengths are listed in Table S6-S7.

Theoretical band calculation: The single crystal data of [TMPDA]₂Pb₃Br₁₀ was directly used to calculate the electronic band structure in Castep software. The total energy was calculated with density functional theory (DFT) using Perdew Burke Ernzerhof (PBE) generalized gradient approximation.²⁹ The interactions between the ionic cores and the electrons were described by the norm-conserving pseudopotential. Hence, the C-2s²2p², N-2s²2p³, H-1s¹, Pb-6s²6p² and Br-4s²4p⁵ orbitals were adopted as valence electrons. The number of plane wave included in the basis sets was determined by a cutoff energy of 320 eV.

Photoluminescent property characterizations: The PL spectra were performed on an Edinburgh FLS980 fluorescence spectrometer. The photoluminescence quantum yield (PLQY) was achieved by incorporating an integrating sphere into the FLS980 spectrofluorometer. The PLQY was calculated based on the equation: $\eta_{QE} = I_S / (E_R - E_S)$, which I_S represents the luminescence emission spectrum of the sample, E_R is the spectrum of the excitation light from the empty integrated sphere (without the sample), and E_S is the excitation spectrum for exciting the sample. The time-resolved decay data were carried out using the Edinburgh FLS980 fluorescence spectrometer with a picosecond pulsed diode laser. The average lifetime was obtained by exponential fitting. The power-dependent photoluminescence spectra were measured using the 375 nm (LE-LS-375-140TFCA, 1-140 mW). The CIE chromaticity coordinates and CRI were calculated using the CIE calculator software based on the emission spectra.

Fabrication of WLED lamp: The WLED lamp device was fabricated by combining a 365 nm UV LED chip with the green phosphor [TMPDA]₂Pb₃Br₁₀, the commercial K₂SiF₆:Mn⁴⁺ red phosphor and the commercial BaMgAl₁₀O₁₇:Eu²⁺ blue phosphor. These three phosphors were mixed with epoxy resin and stirred continuously for 10 min. Then the mixture was coated on the surface of the UV LED chip and cured for 30 min under vacuum conditions. The optical properties of the

fabricated WLED was evaluated by a temperature-programmed LED optoelectronic analyzer with an integrating sphere (EVERFINE HAAS-2000).

Preparation of the [TMPAD]₂Pb₃Br₁₀ film: 0.30 g sample powder was dissolved in 1 mL of ethanol (EA) to obtain the homogeneous suspension solution; and 0.5 g polyethylene pyrrolidone (PVP) was then placed into the above solution and stirred at room temperature for 4 h to produce a light green viscous liquid. To prepare the film, a small amount of the viscous liquid was taken and spun on a spinner at the speed of 2100 rap/min; then a thin [TMPAD]₂Pb₃Br₁₀ film was obtained.

Preparation of the [TMPAD]₂Pb₃Br₁₀-PVDF composites: 0.10 g powder sample was dissolved in 1 mL of N, N-dimethylformamide (DMF) to obtain the homogeneous suspension solution; and 0.3 g polyvinylidene fluoride (PVDF) were then placed into the above solution and stirred at room temperature for 1 h to produce a light green viscous liquid. A certain amount of the above-mentioned viscous liquid was taken by a dropper and then added into a 500 mL beaker filled with 200 mL of water one by one. The settled balls were obtained at the bottom of the beaker. The minimum concentration of PVDF for fluorescent ball formation is 0.15 g/mL with the minimum ratio of 1:5 between [TMPAD]₂Pb₃Br₁₀ and PVDF.

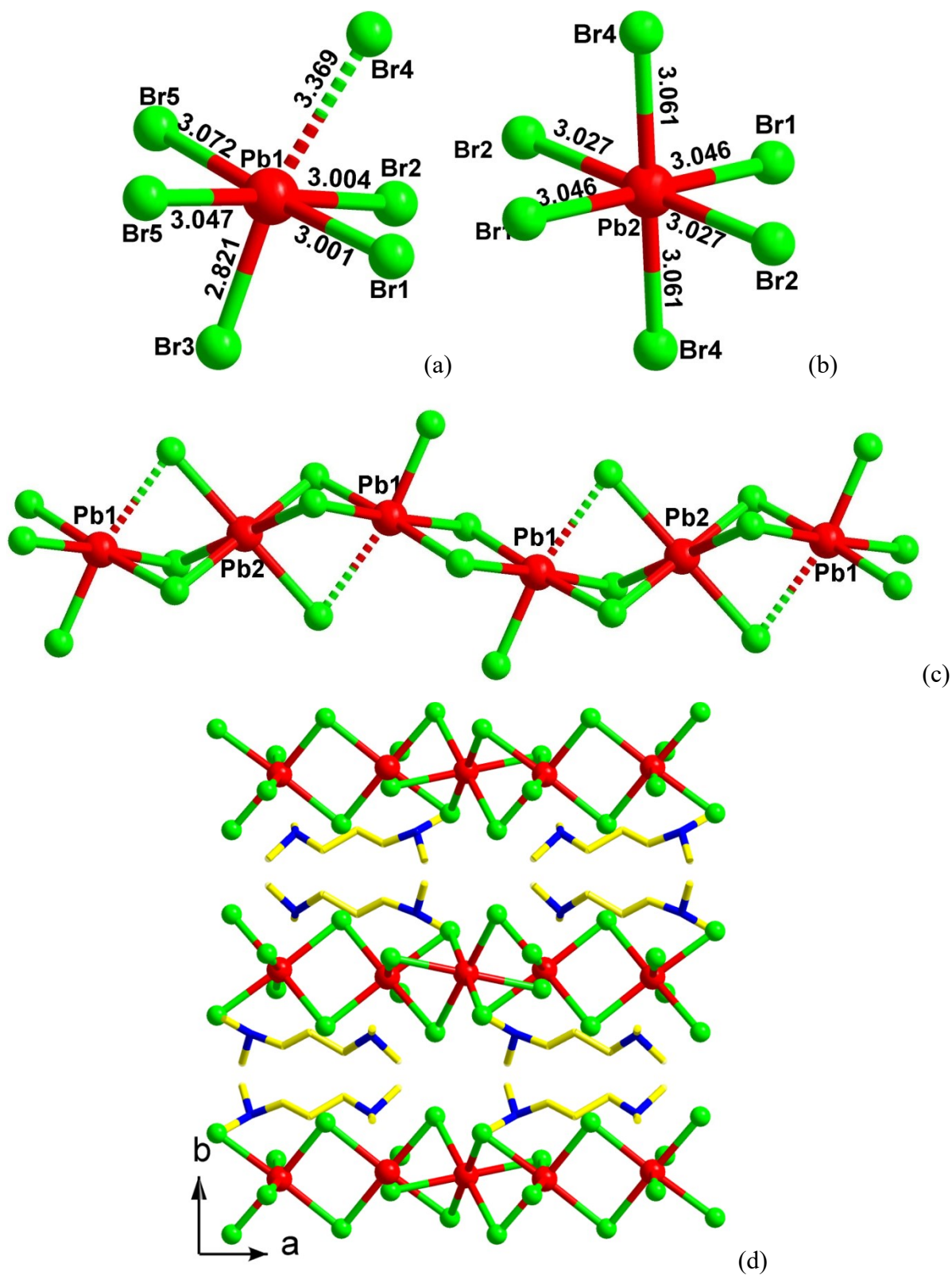


Figure S1. The coordination environments of Pb1 (a) and Pb2 (b) atoms, schematic of 1D $[\text{Pb}_3\text{Br}_{10}]^{4-}$ chain (c) and the packing framework along the c -axis (d) of compound $[\text{TMPDA}]_2\text{Pb}_3\text{Br}_{10}$.

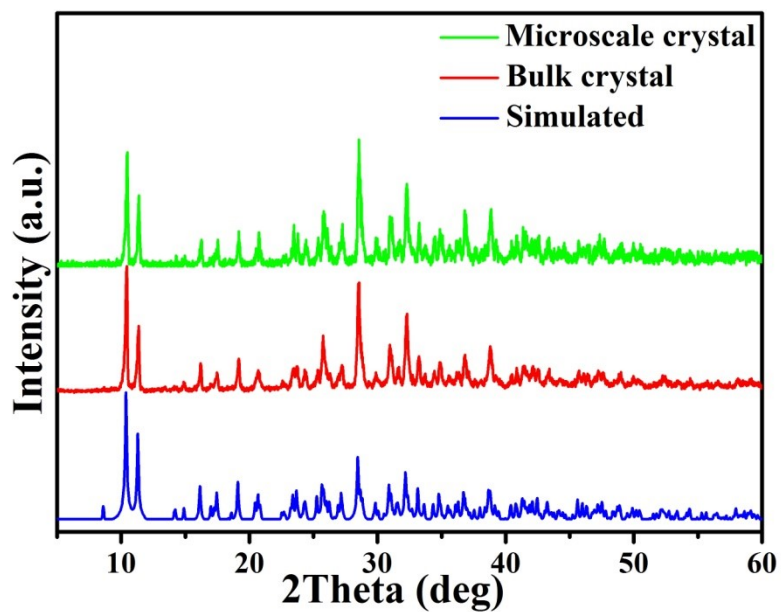


Figure S2. The PXR D patterns of bulk and microscale crystals of $[\text{TMPDA}]_2\text{Pb}_3\text{Br}_{10}$ as well as simulated data from single crystal structure.

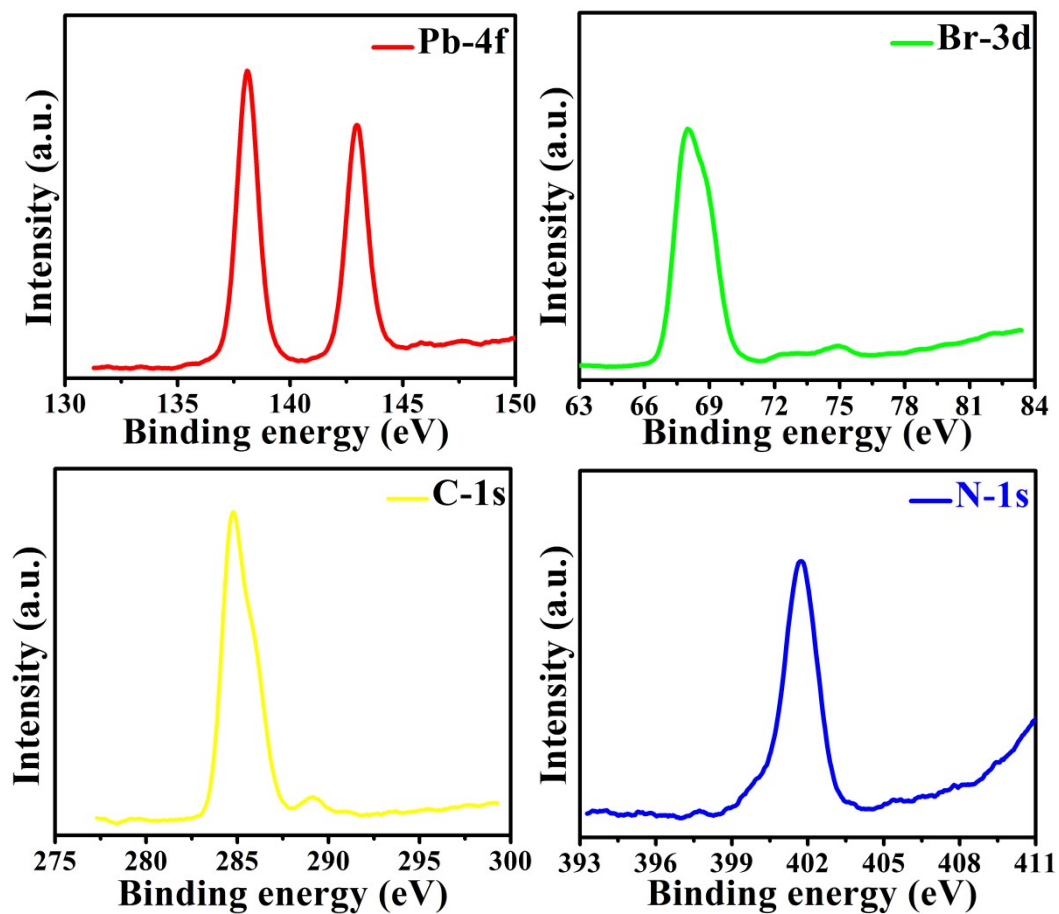


Figure S3. The XPS spectra of Pb, Br, C and N atoms in $[\text{TMPDA}]_2\text{Pb}_3\text{Br}_{10}$.

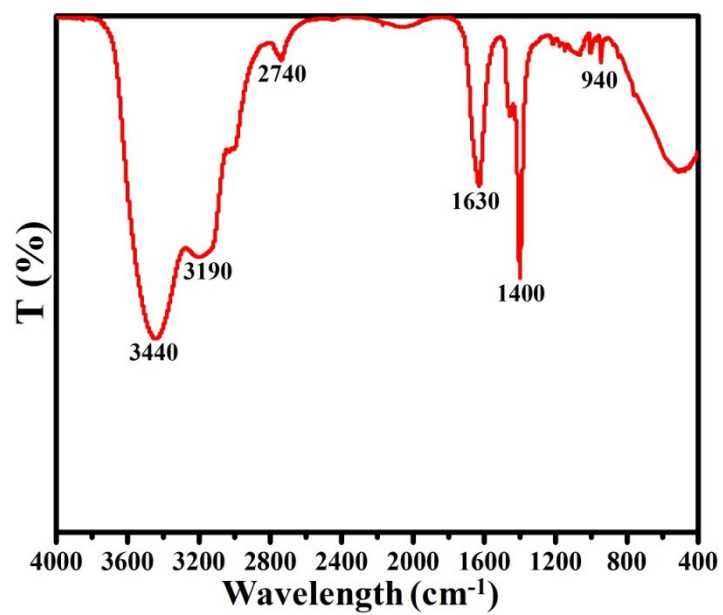
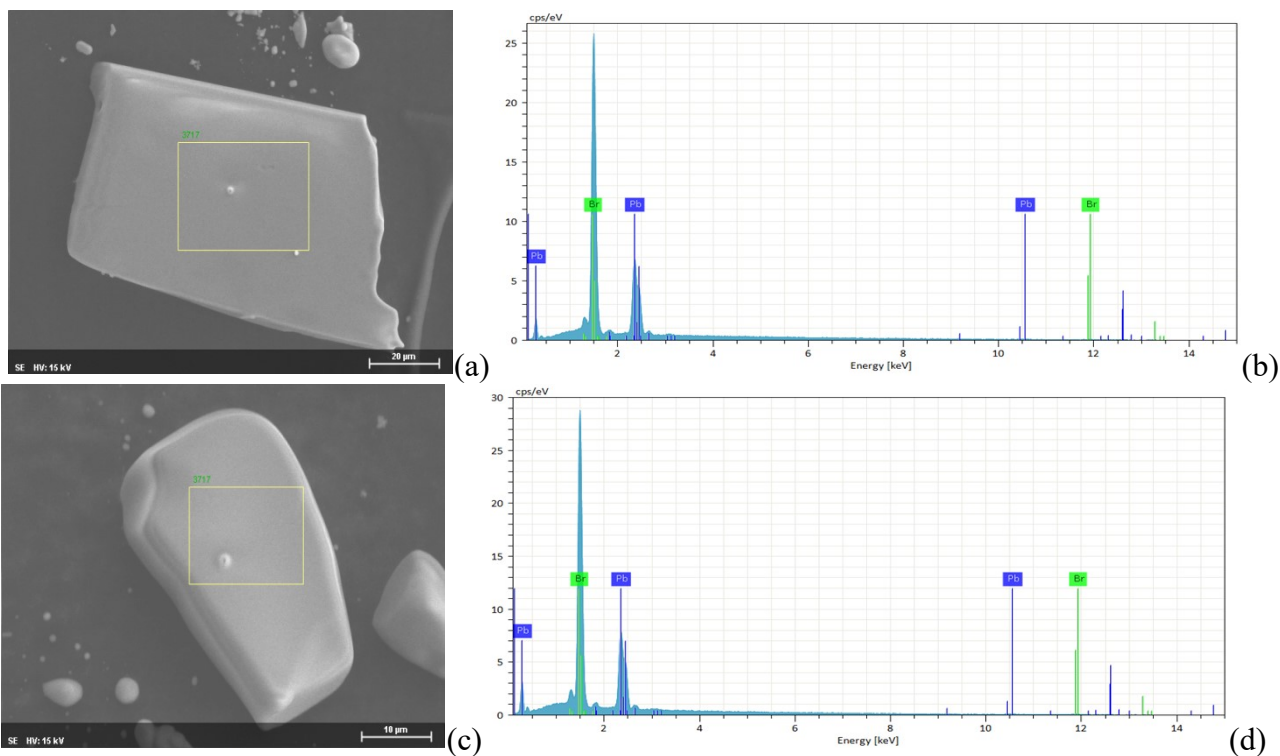


Figure S4. The IR spectrum of compound [TMPDA]Pb₃Br₁₀.



1.xlsx

Element	At. No.	Line s.	Netto	Mass [%]	Mass Norm. [%]	Atom [%]	abs. error [%] (1 sigma)	abs. error [%] (2 sigma)	abs. error [%] (3 sigma)	rel. error [%] (1 sigma)	rel. error [%] (2 sigma)	rel. error [%] (3 sigma)
Bromine	35	L-Series	110032	52.44	58.88	78.78	2.47	4.94	7.41	4.71	9.42	14.13
Lead	82	M-Series	44458	36.62	41.12	21.22	1.33	2.66	3.99	3.64	7.27	10.91
			Sum	89.05	100.00	100.00						

(e)

2.xlsx

Element	At. No.	Line s.	Netto	Mass [%]	Mass Norm. [%]	Atom [%]	abs. error [%] (1 sigma)	abs. error [%] (2 sigma)	abs. error [%] (3 sigma)	rel. error [%] (1 sigma)	rel. error [%] (2 sigma)	rel. error [%] (3 sigma)
Bromine	35	L-Series	117271	46.49	57.20	77.61	2.19	4.38	6.58	4.72	9.43	14.15
Lead	82	M-Series	48277	34.78	42.80	22.39	1.26	2.53	3.79	3.64	7.27	10.91
			Sum	81.28	100.00	100.00						

(f)

Figure S5. The SEM photos (a and c) and corresponding EDX spectrum (b and d) as well as the contents of lead and bromine elements (e and f) for bulk crystals of $[\text{TMPDA}]_2\text{Pb}_3\text{Br}_{10}$.

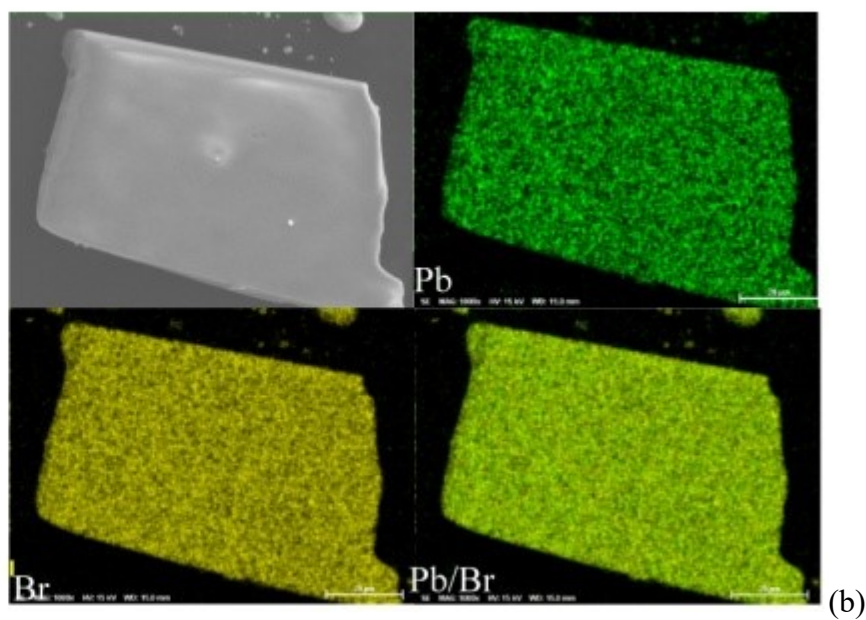
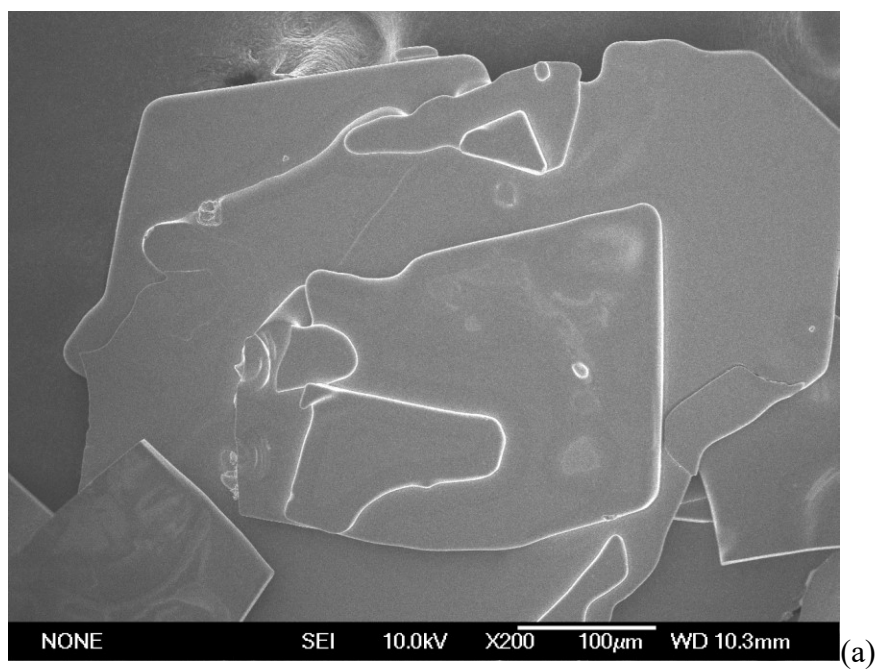


Figure S6. The SEM photos of single crystals (a) and EDX elemental mapping images of Pb and Br elements of $[\text{TMPDA}]_2\text{Pb}_3\text{Br}_{10}$.

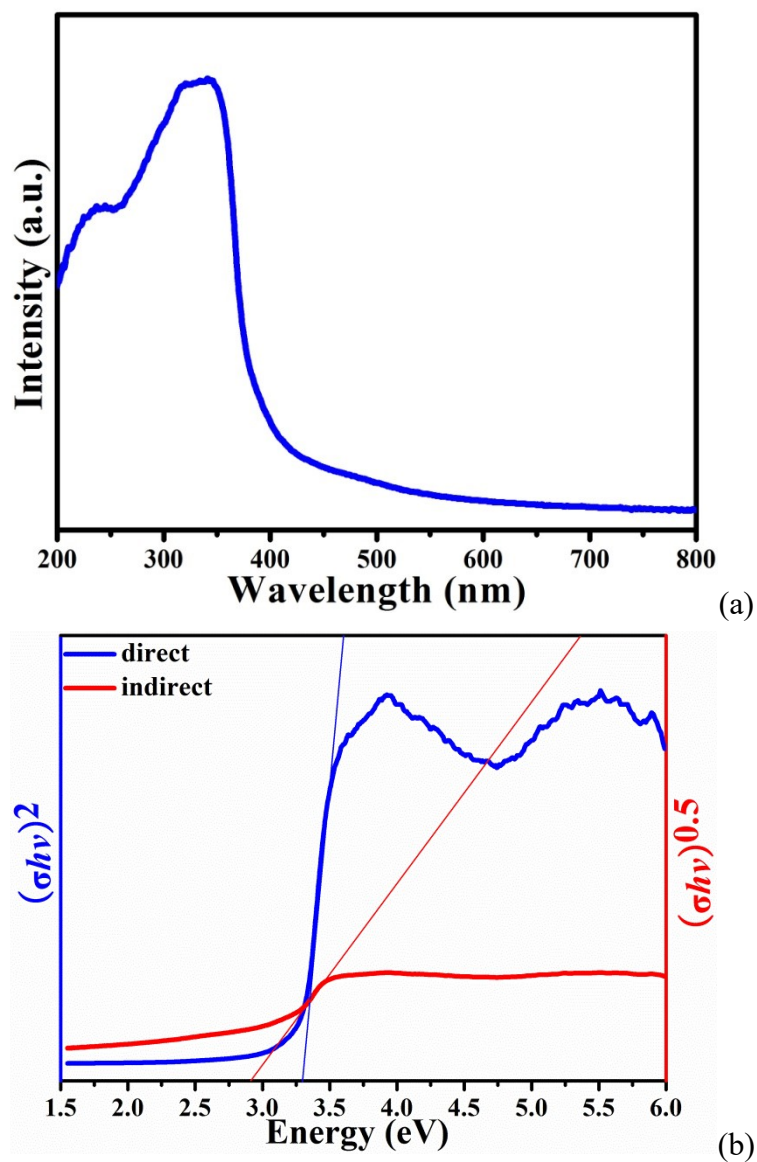


Figure S7. (a) The solid-state UV-Vis absorption spectrum of $[\text{TMPDA}]_2\text{Pb}_3\text{Br}_{10}$, (b) the Tauc plots based on the assumptions of direct and indirect transitions.

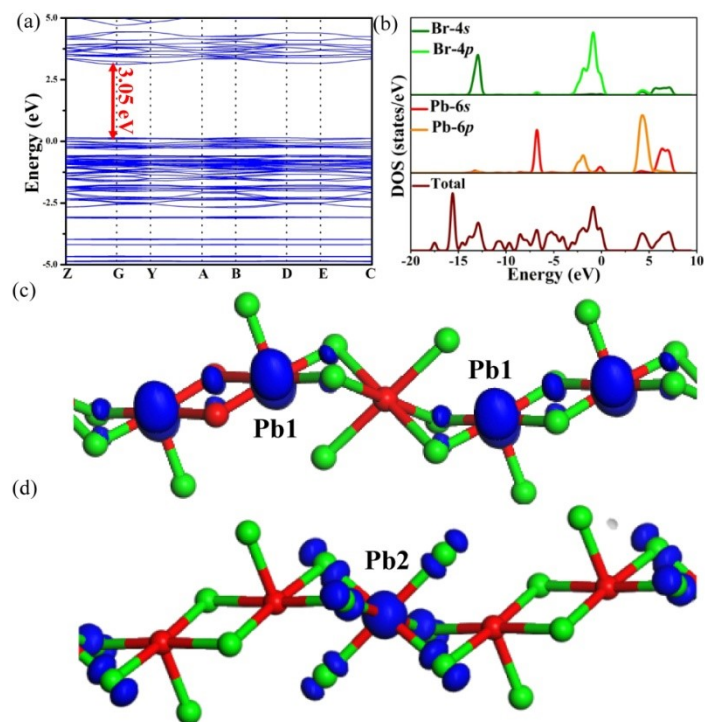


Figure S8. The calculated electronic band structure (a), total and partial density of states (b), charge density of lowest unoccupied molecular orbital (c) and highest occupied molecular orbital (d) for $[\text{TMPDA}]_2\text{Pb}_3\text{Br}_{10}$.

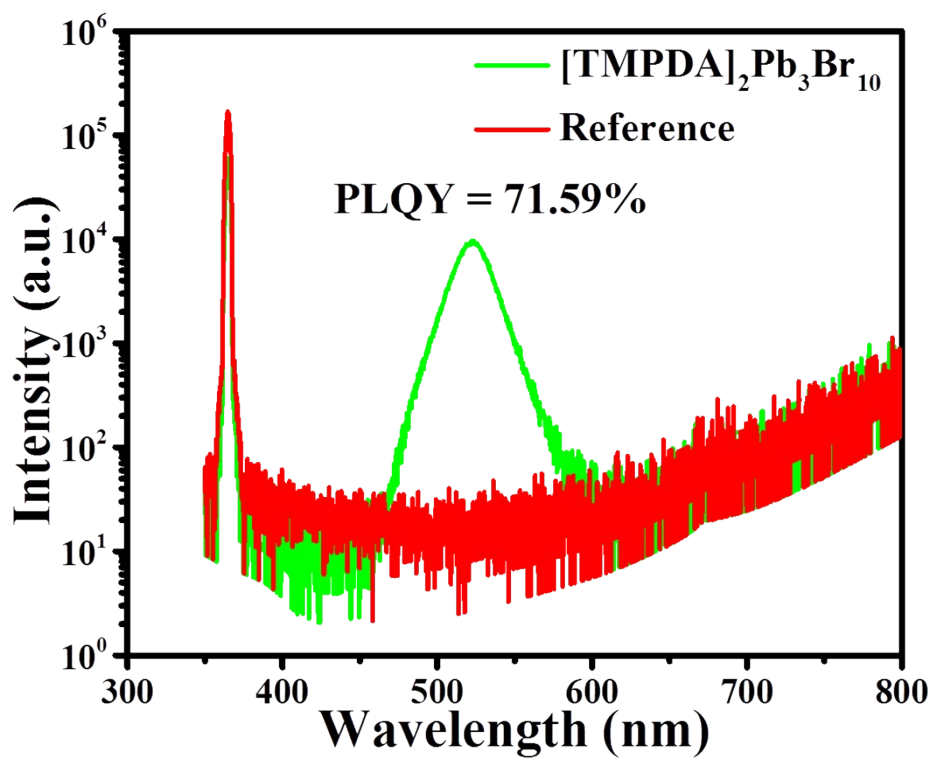


Figure S9. The PLQY of bulk crystals for compound $[\text{TMPDA}]_2\text{Pb}_3\text{Br}_{10}$.

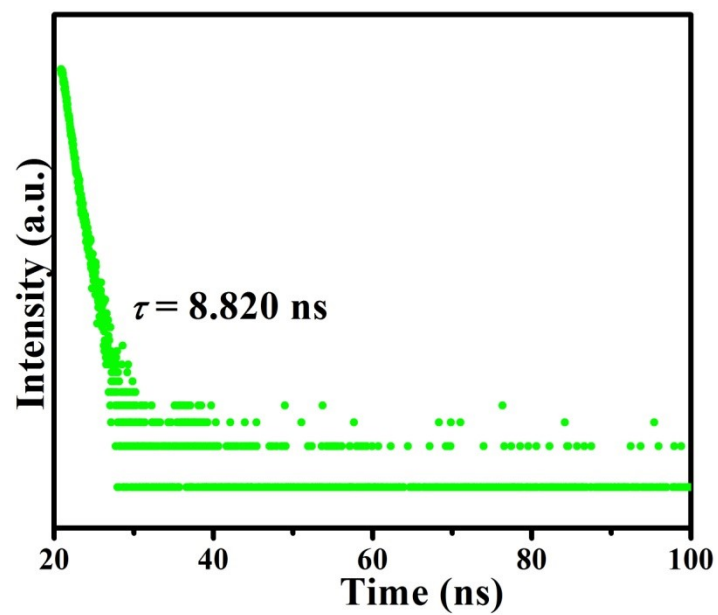


Figure S10. The time-resolved PL decay curve of [TMPDA]₂Pb₃Br₁₀ bulk crystals at 100 K.

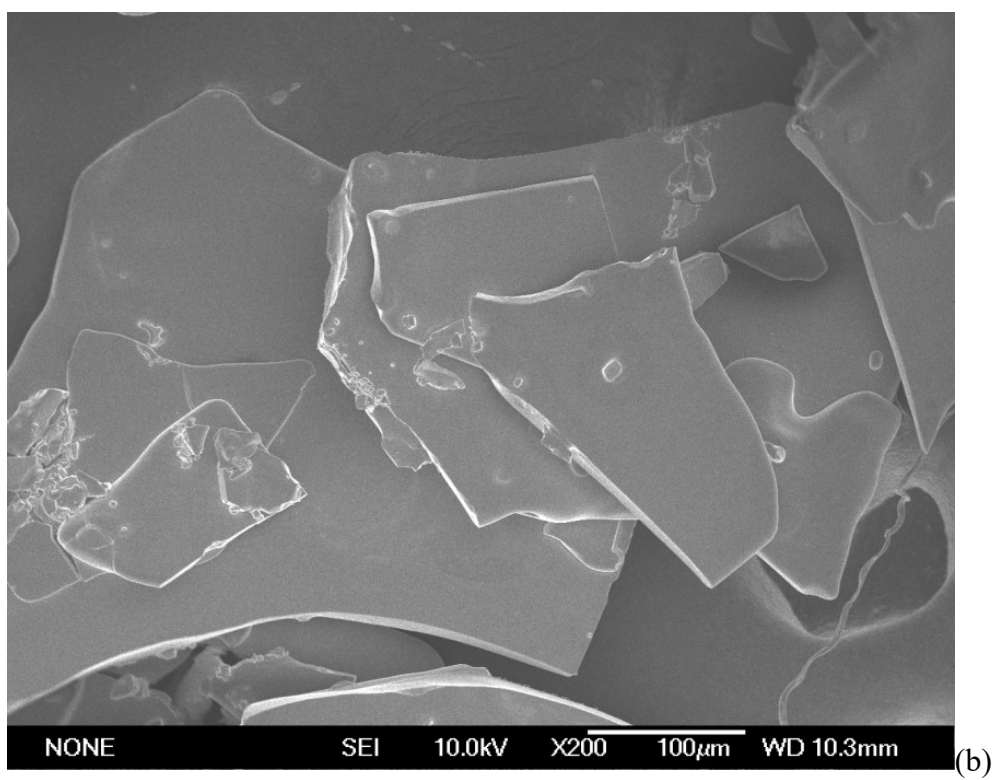
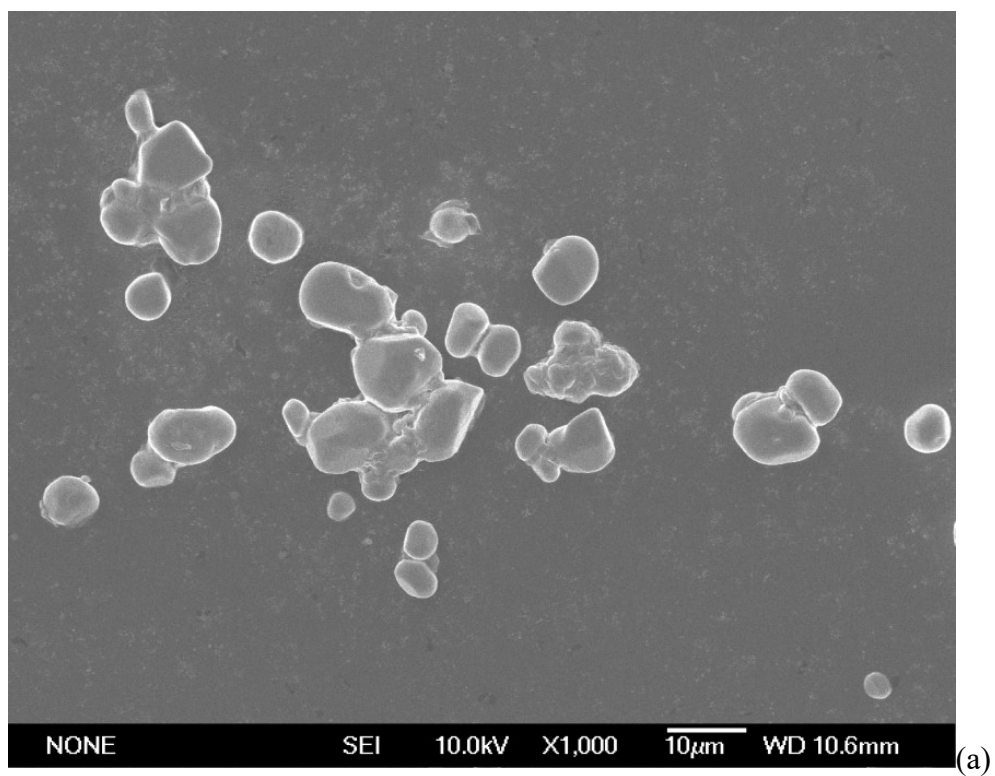


Figure S11. The SEM photos of microscale crystals (a) and bulk crystals (b) of $[\text{TMPDA}]_2\text{Pb}_3\text{Br}_{10}$.

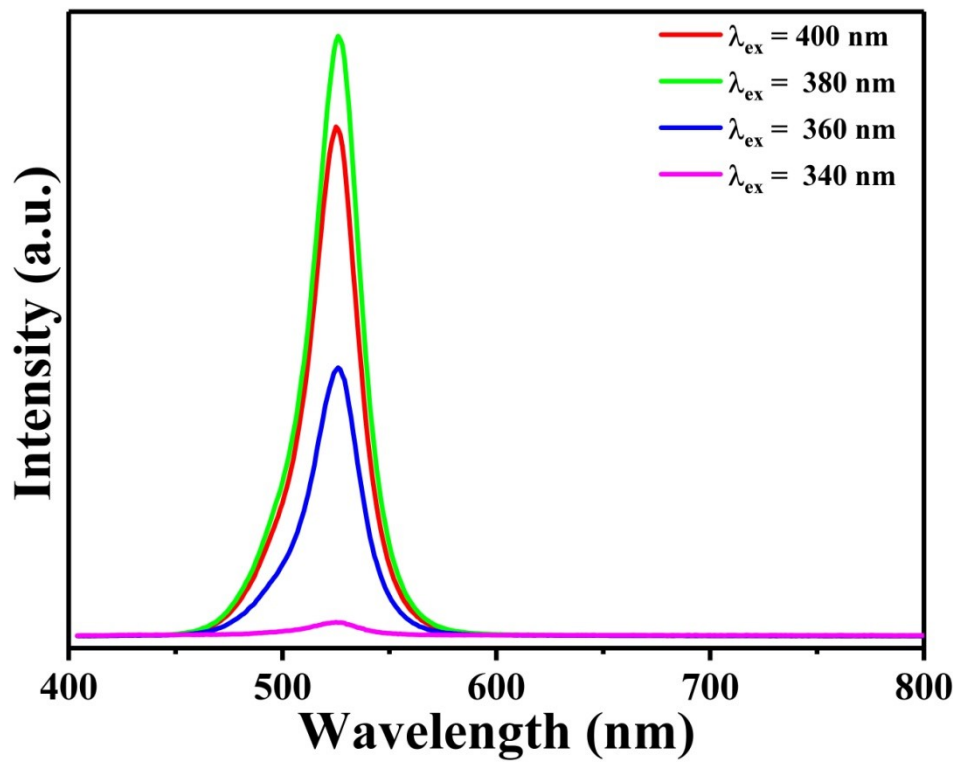


Figure S12. The excitation wavelength dependent PL emission spectra of compound [TMPDA]₂Pb₃Br₁₀ at 300 K.

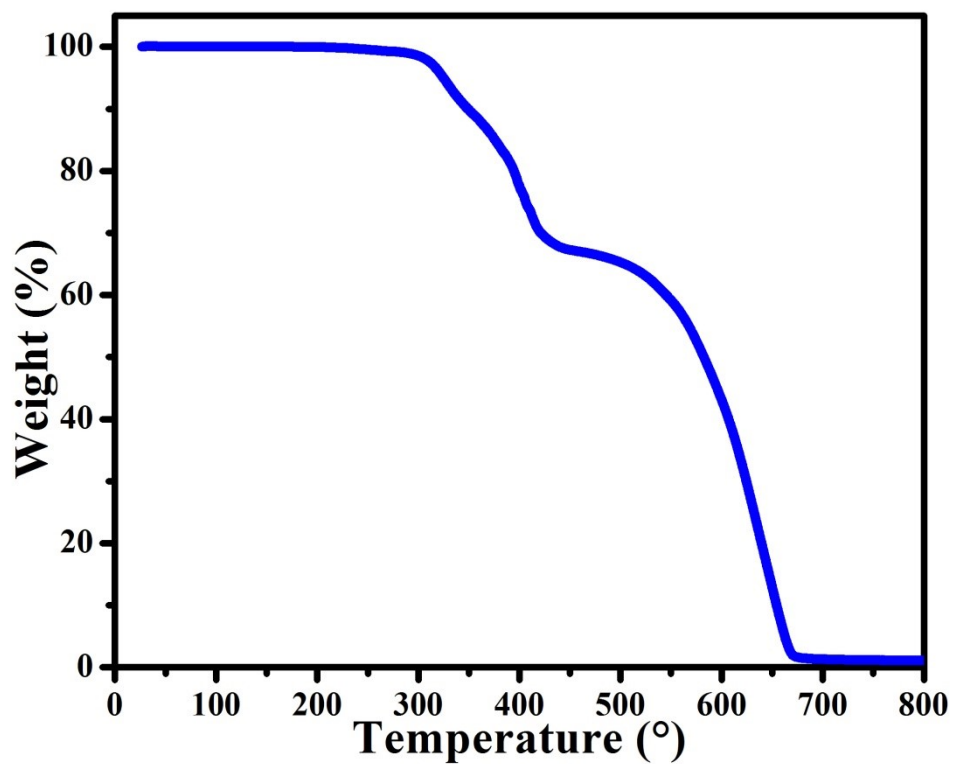


Figure S13. The thermogravimetric analysis curve for $[\text{TMPDA}]_2\text{Pb}_3\text{Br}_{10}$.

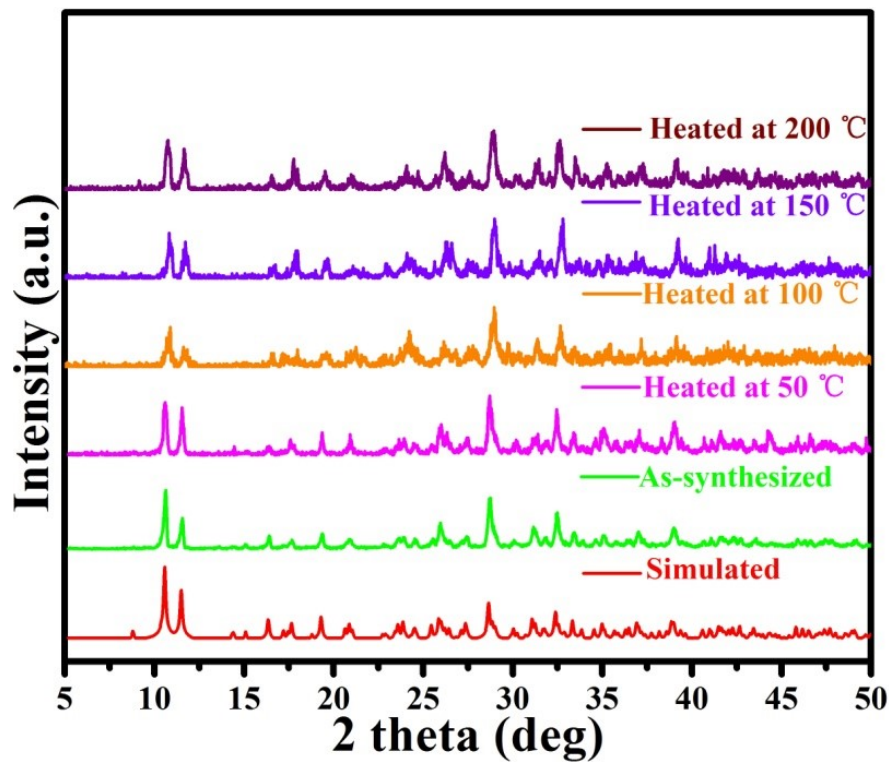


Figure S14. Comparison of the PXR D patterns of $[\text{TMPDA}]_2\text{Pb}_3\text{Br}_{10}$ before and after heating at various temperature from 50 °C to 200 °C.

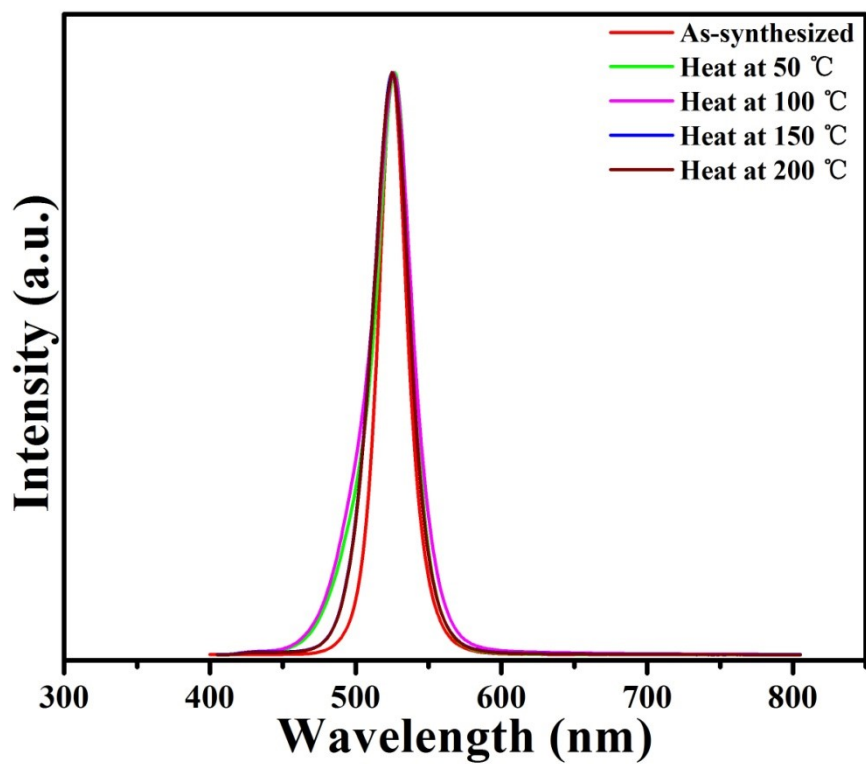


Figure S15. Comparison of the normalized PL emission spectra of [TMPDA]₂Pb₃Br₁₀ before and after heating from 50 °C to 200 °C.

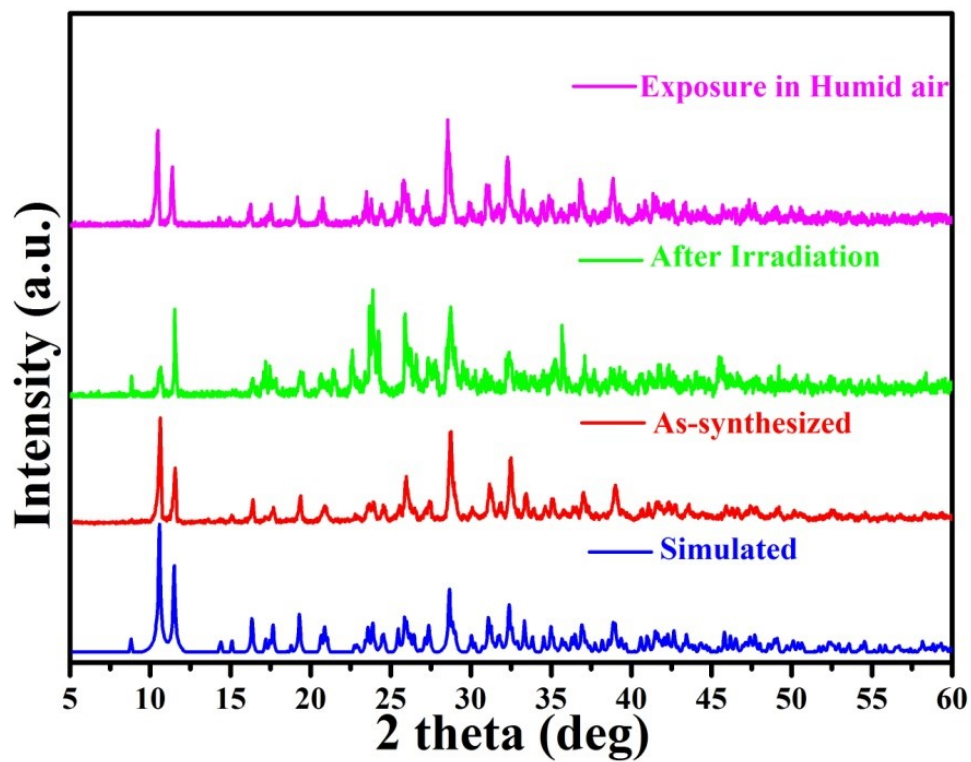


Figure S16. The PXRD patterns of $[\text{TMPDA}]_2\text{Pb}_3\text{Br}_{10}$ before and after storing in humid air (>90%) or exposure under UV light irradiation.

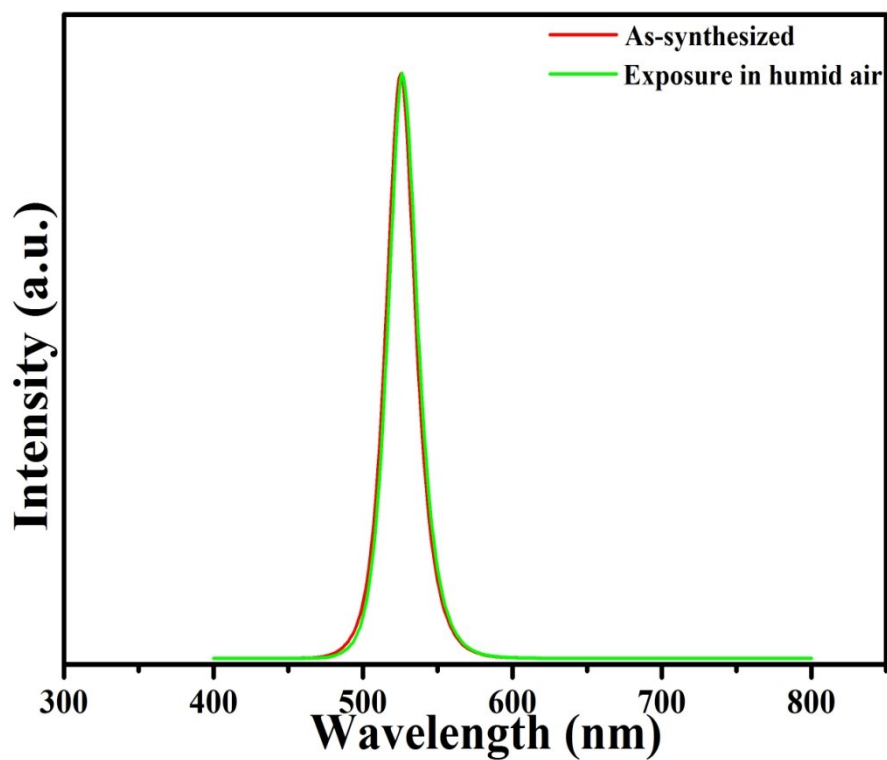


Figure S17. Comparison of the normalized PL emission spectra of [TMPDA]₂Pb₃Br₁₀ before and after exposure in humid air for one year at room temperature.

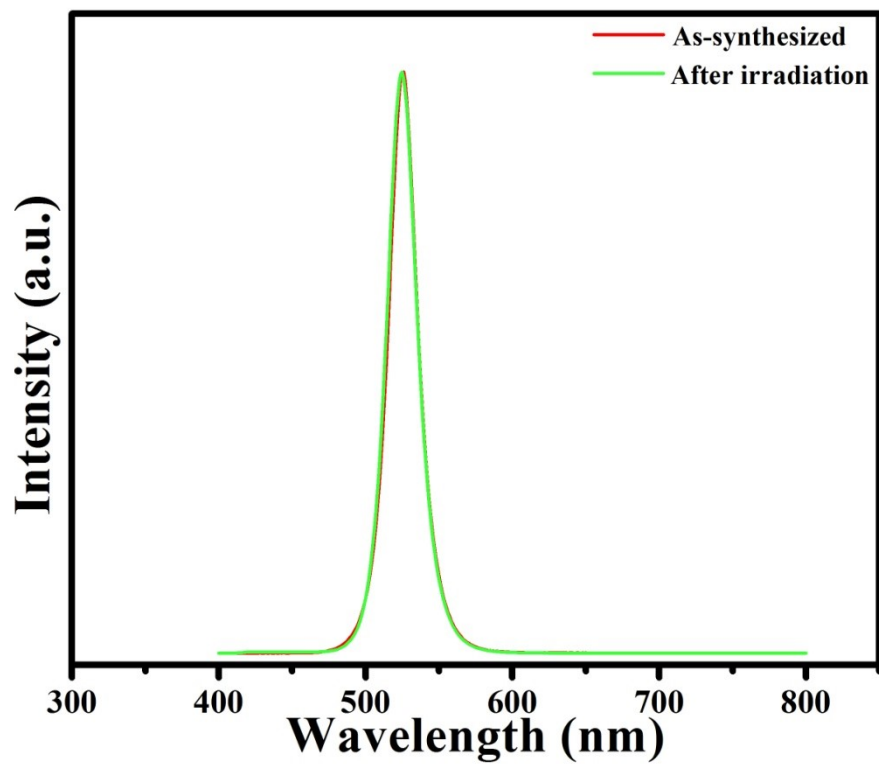


Figure S18. Comparison of the normalized PL emission spectra of [TMPDA]₂Pb₃Br₁₀ before and after exposure in UV light irradiation for 48 hours at 300 K.

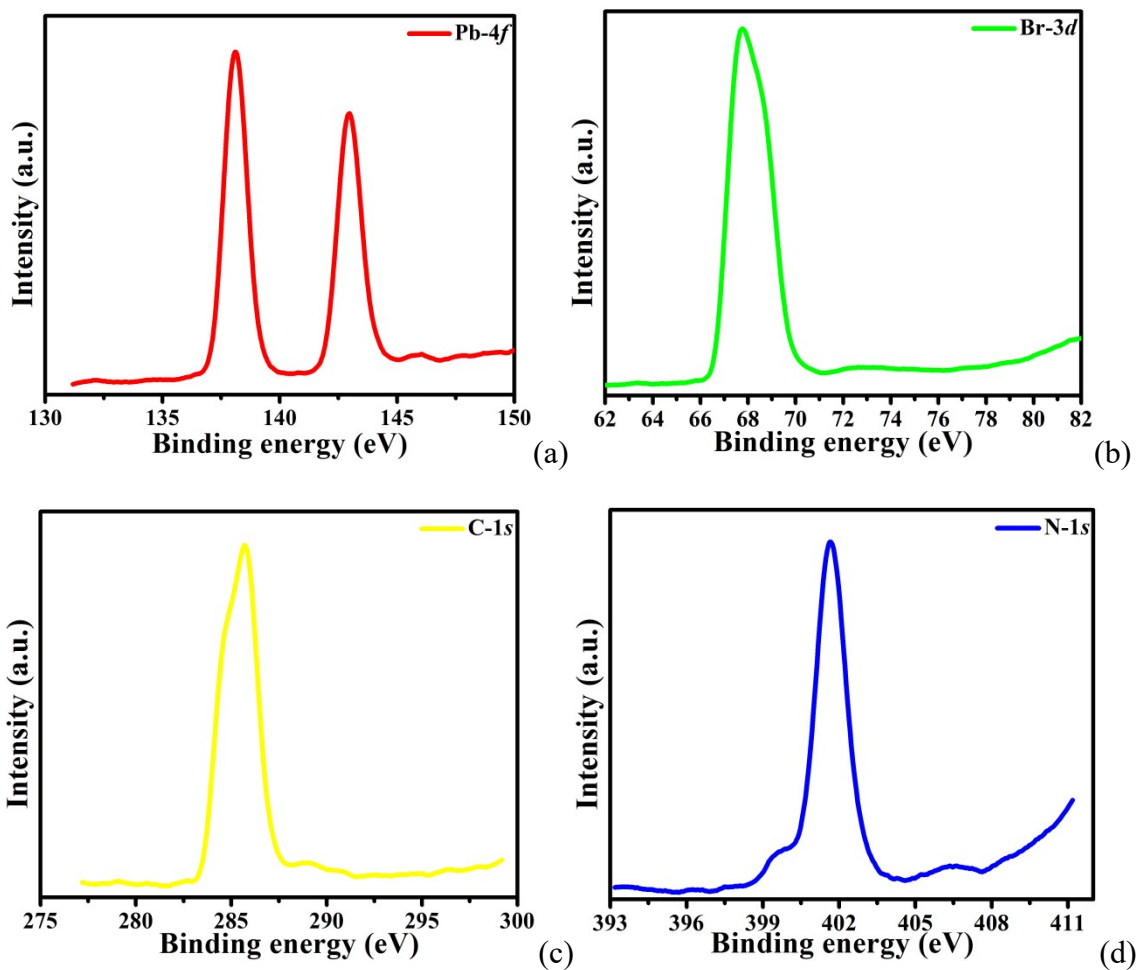


Figure S19. The XPS spectra of Pb, Br, C and N atoms for [TMPDA]₂Pb₃Br₁₀ after long-term exposure under strong UV-light irradiation.

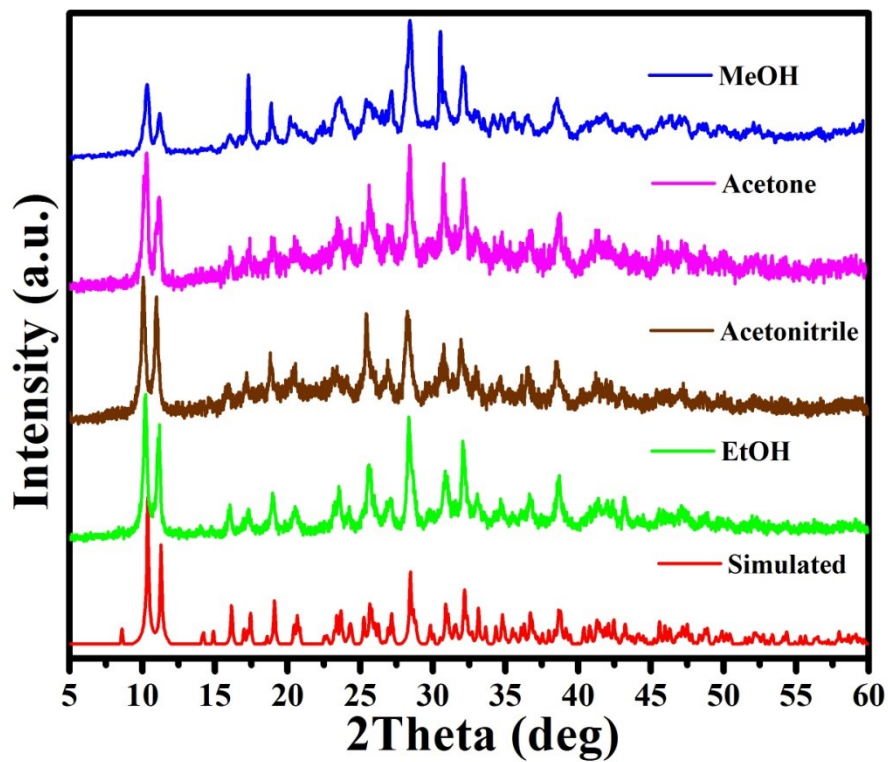


Figure S20. The PXRD patterns of $[\text{TMPDA}]_2\text{Pb}_3\text{Br}_{10}$ after soaking in various organic solvents for one day.

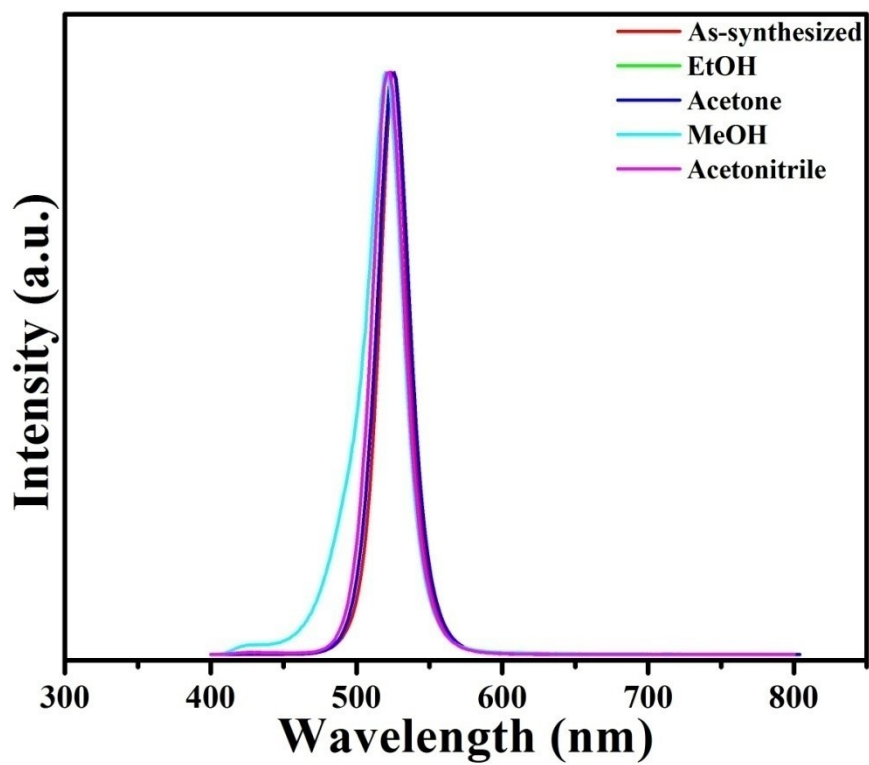


Figure S21. The PL emission spectra of [TMPDA]₂Pb₃Br₁₀ before and after soaking in various organic solvents for one day.

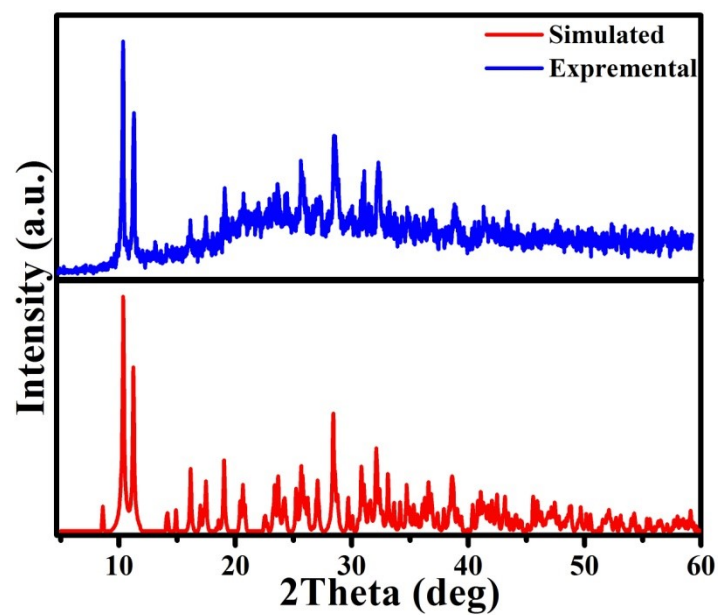


Figure S22. The experimental powder X-ray diffraction data of prepared $[\text{TMPDA}]_2\text{Pb}_3\text{Br}_{10}$ film and simulated data.

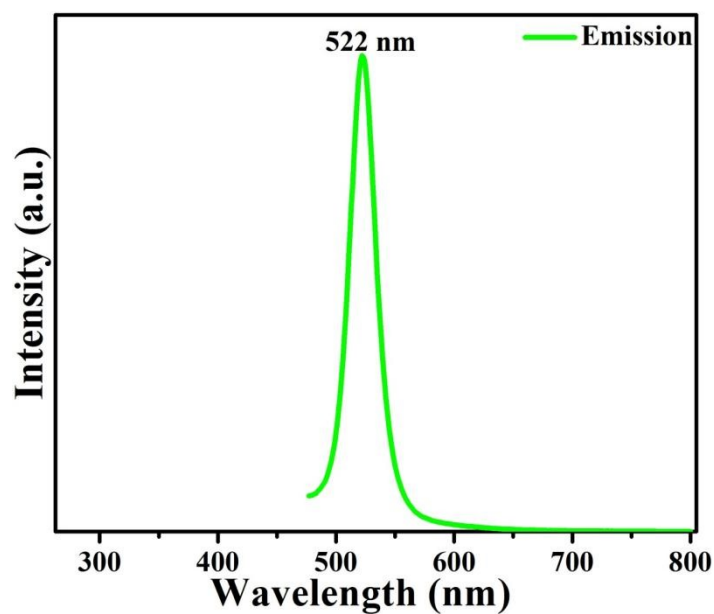


Figure S23. The PL emission spectrum of prepared $[\text{TMPDA}]_2\text{Pb}_3\text{Br}_{10}$ based film at 300 K.

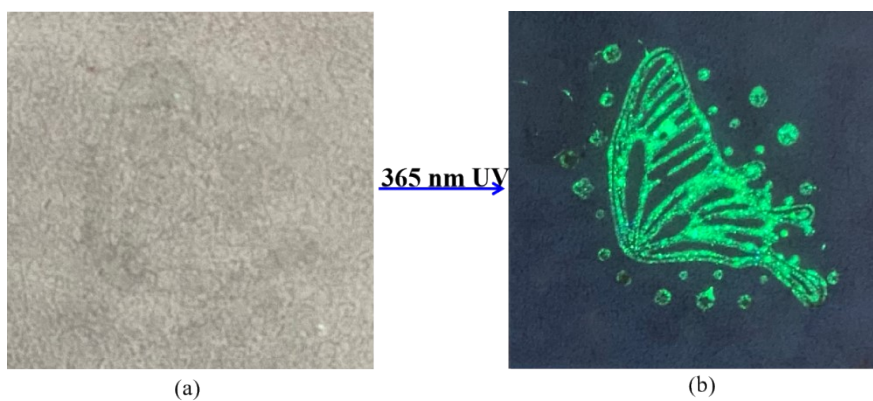


Figure S24. Anti-counterfeiting application of $[\text{TMPDA}]_2\text{Pb}_3\text{Br}_{10}$: the photo images of printed patterns on commercial parchment paper under ambient light (a) and a 365 nm UV lamp (b).

Table S1. Summary of the photoluminescence parameters of green light emitting metal halides.

Material	Emission (nm)	CIE	PLQY	FWHM (nm)	CP*	Lifetime	Ref.
Single Crystalline Lead halides							
[bmpy] ₉ [ZnCl ₄] ₂ [Pb ₃ Cl ₁₁]	512	(0.16,0.55)	100%	61.3	53.38%	0.54 μs	1
[bmpy] ₉ Pb ₃ Zn ₂ Cl ₁₉	516	(0.19, 0.60)	91%	61	54.33%	569 ns	2
[TMPDA]₂Pb₃Br₁₀	526	(0.16, 0.77)	71.59%	25	91.1%	3.58 ns	This work
[bmpy] ₉ [MnBr ₄] ₂ [Pb ₃ Br ₁₁]	528	(0.29, 0.65)	49.8%	67	82.73%	114.3 μs	3
[bmpy] ₆ Pb ₃ Br ₁₂	522	(0.26, 0.39)	12%	134	20.31%	36.78 ns	4
[bmpy] ₉ [ZnBr ₄] ₂ [Pb ₃ Br ₁₁]	564	(0.40, 0.53)	7%	68	79.60%	36 ns	5
Single Crystalline Maganese halides							
(TMPEA) ₂ MnBr ₄	520	-	98%	-	-	96 μs	6
(ETPP)MnBr ₄	517	-	95%	51	-	318 μs	7
[P14]MnBr ₄	520	(0.23, 0.68)	81%	55	77.73%	358 μs	8
(Bmpy) ₂ MnBr ₄	528	(0.28, 0.65)	80.1%	64	79.23%	326 μs	9
(MPip)MnCl ₄	530	-	79.4	60	-	715 μs	10
(Bz(Me) ₃ N) ₂ MnCl ₄	547	-	78 %	71.8	-	3.79 ms	11
(C ₇ H ₁₃ N ₂) ₂ MnCl ₄	536	(0.24, 0.38)	70.8	-	29.76%	3.9 ms	12
[PP14]MnBr ₄	527	(0.28, 0.66)	55%	64	82.91%	361 μs	8
Cs ₃ MnBr ₅	520	(0.15, 0.76)	49%	42	78.98%	0.29 ms	13
(TPP) ₂ MnCl ₄	517	-	48%	-	-	1.97 ms	14
(Mor) ₂ MnCl ₄	520	(0.24,0.64)	39 %	-	69.71%	3.36 ms	15
Perovskite Quantum Dots or Nanomaterials							
CsPbBr ₃	507	(0.23, 0.63)	80%	23	64.56%	6.6 ns	16
MAPbBr ₃ film	532	(0.25, 0.74)	-	15.3	98.1%	15.28 ns	17
FAPbBr ₃ nanoplate	530	(0.17,0.76)	85%	25.3	95%	12 ns	18
FAPbBr ₃ film	530	(0.17, 0.77)	92%	22	97%	24.2 ns	19
Cs ₃ Cu ₂ Cl ₅	515	(0.19, 0.42)	91.3%	91	43.24%	112.4 μs	20

*CP represents the color purity.

Bmpy = 1-butyl-1-methylpyrrolidinium; TMPEA = trimethylphenylammonium; ETPP = ethylenebis-triphenylphosphonium; P14 = N-butyl-N-methylpyrrolidinium, MPip = N-methylpiperidinium, Bz(Me)₃N = N-benzyl-N,N,N-trimethylammonium; [EMMI] = 1-ethyl-2,3-dimethylimidazolium chloride; PP14 = N-butyl-N-methylpiperidinium; TPP = tetraphenylphosphonium, Mor = morpholine.

Table S2. Summary of the green light emissions of representative commercial inorganic green phosphors.

Material	Emission	CIE	PLQY	FWHM	CP	Lifetime	Ref.
β -SiAlON:Eu ²⁺	538 nm	(0.24, 0.63)	96.5%	53 nm	59.12%	1 μ s	21
MgAl ₂ O ₄ :Mn ²⁺	525 nm	(0.20, 0.74)	45%	35 nm	89.61%	6.51 ms	22
Sr ₂ MgAl ₂₂ O ₃₆ :Mn ²⁺	518 nm	(0.150, 0.77)	75%	26 nm	81.5%	4.71 ms	23
Ba[Li ₂ (Al ₂ Si ₂)N ₆]:Eu ²⁺	532 nm	(0.30, 0.64)	80%	57 nm	83.93%	-	24
Ba ₂ LiSi ₇ AlN ₁₂ :Eu ²⁺	515nm	(0.24, 0.61)	79%	61 nm	60.30%	0.6 μ s	25
RbLi(Li ₃ SiO ₄) ₂ :Eu ²⁺	530 nm	(0.21, 0.72)	80%	42 nm	86.32%	-	26
SrGa ₂ S ₄ :Eu ²⁺	540 nm	(0.32, 0.63)	95%	47 nm	85.78%	-	27

Table S3. The comparison of calculated Huang-Rhys factors for various luminescent materials.

Compounds	Huang-Rhys factor	Reference
ZnSe	0.3	<i>Phys. Rev. B</i> 2003 , 68, 125309.
CdSe	1	<i>Phys. Rev. B</i> 2000 , 61, 9944.
[TMPDA] ₂ Pb ₃ Br ₁₀	1.57	This work
CsPbBr ₃	3.223	<i>Nanoscale</i> , 2018 , 10, 9949–9956.
FAPbBr ₃	<3.3	
MAPbBr ₃	<3.3	
CsSnI ₃	<3.3	
Cs ₂ SnI ₆	4.9	<i>Phys. Rev. Applied.</i> 2020 , 14, 014048
SrSe	6.4	<i>Jpn. J. Appl. Phys.</i> 1995 , 34, 5539–5545.
Cs ₂ NaYCl ₆	7.0	<i>Phys. Rev. B</i> 1986 , 34, 2735.
Y ₃ Al ₅ O ₁₂	8.4	<i>Chem. Mater.</i> 2009 , 21, 2077–2084.
Lu ₃ Al ₅ O ₁₂	9.0	<i>J. Phys. Chem. A.</i> 2012 , 116, 8464–8474.
Cs ₂ AgBiBr ₆	11.7	<i>J. Mater. Chem. C.</i> 2019 , 7, 8350.
Sb ³⁺ :Cs ₂ NaInCl ₆	11.96	<i>J. Phys. Chem. Lett.</i> 2020 , 11, 2053–2061.
(PMA) ₃ SbBr ₆	12.5	<i>J. Mater. Chem. C</i> 2020 , 8, 7322–7329.
(PMA) ₃ BiBr ₆	13.7	
Cs ₂ AgBiBr ₆	15.4	<i>ACS Nano.</i> 2018 , 12, 8081–8090.
Cs ₂ AgInCl ₆	37	<i>Nature</i> 2018 , 563, 541–545.
Rb ₂ CuBr ₃	37.17	<i>Adv. Mater.</i> 2019 , 1904711.
Cs ₂ Ag _{0.6} Na _{0.4} InCl ₆	40.9	<i>Nature</i> 2018 , 563, 541–545.
Cs ₃ Sb ₂ I ₉	42.7	<i>Chem. Mater.</i> 2017 , 29, 4129–4145.
Rb ₃ Sb ₂ I ₉	50.4	
Cs ₂ Ag _{0.16} Na _{0.84} InCl ₆	51.0	<i>Nature</i> 2018 , 563, 541–545.
Cs ₃ Bi ₂ I ₉	79.5	<i>Chem. Mater.</i> 2017 , 29, 4129–4145.
Cs ₂ NaInCl ₆	80 (ES)/188 (GS)	<i>Nature</i> 2018 , 563, 541–545.
Cs ₃ Bi ₂ I ₆ Cl ₃	212	<i>Chem. Mater.</i> 2019 , 31, 2644–2650.

Table S4. Comparison of color gamut in CIE 1931 color space of fabricated WLED based on green light emitting phosphors.

Material	NTSC	Reference
$\text{Sr}_2\text{MgAl}_{22}\text{O}_{36}:\text{Mn}^{2+}$	127%	<i>Adv. Opt. Mater.</i> 2018 , 1801419.
CsPbBr_3 QD@glass	125%	<i>J. Mater. Chem. C.</i> 2019 , 7, 13139–13148.
[TMPDA]₂Pb₃Br₁₀	121.5%	This work
$\text{MgAl}_2\text{O}_4:\text{Mn}^{2+}$	116%	<i>J. Mater. Chem. C.</i> 2019 , 7, 8192–8198.
$\text{Al}@\text{CsPbBr}_3$	116%	<i>Adv. Sci.</i> 2017 , 4, 1700335.
$\text{RbLi}(\text{Li}_3\text{SiO}_4)_2:\text{Eu}^{2+}$	107%	<i>Adv. Mater.</i> 2018 , 30, 1802489.
$\text{h-BN}@\text{(PMA)}_2\text{MA}_{n-1}\text{Pb}_n\text{Br}_{3n+1}$	106.1%	<i>ACS Appl. Mater. Interfaces</i> 2020 , 12, 27386–27393.
Cs_3MnBr_5	104%	<i>J. Mater. Chem. C.</i> 2019 , 7, 11220–11226.
$(\text{C}_{10}\text{H}_{16}\text{N})_2\text{MnBr}_4$	104%	<i>J. Phys. Chem. Lett.</i> 2020 , 11, 5956–5962.
FAPbBr_3	102%	<i>Adv. Funct. Mater.</i> 2018 , 18, 1800248.
CsPbBr_3	102%	<i>Chem. Mater.</i> 2016 , 28, 8493–8497.
$\gamma\text{-AlON}:\text{Mn}^{2+}, \text{Mg}^{2+}$	102%	<i>Jpn. J. Appl. Phys.</i> 2017 , 56, 041701.
$\text{Cs}_3\text{Mn}_{0.96}\text{Zn}_{0.04}\text{Br}_5$	101%	<i>J. Mater. Chem. C.</i> 2019 , 7, 11220–11226.
$\text{Na}[(\text{UO}_2)_2\text{B}_6\text{O}_{10}(\text{OH})]\cdot 2\text{H}_2\text{O}$	95%	<i>Chem. Mater.</i> 2019 , 31, 9684–9690.
$[\text{bmpy}]_9[\text{MnBr}_4]_2[\text{Pb}_3\text{Br}_{11}]$	92.7%	<i>Angew. Chem. Int. Ed.</i> 2019 , 58, 18670–18675.
$\text{SrGa}_2\text{S}_4:\text{Eu}^{2+}$	90%	<i>Opt. Lett.</i> 2013 , 38, 3298.
$\beta\text{-SiAlON}:\text{Eu}^{2+}$	89%	<i>Chem. Mater.</i> 2016 , 28, 8493–8497.
$\beta\text{-Sialon}:\text{Eu}^{2+}$	85.9%	<i>Jpn. J. Appl. Phys.</i> 2016 , 55, 42102.
$\text{Sr}_2\text{SiO}_4:\text{Eu}^{2+}$	74.7%	<i>Opt Express.</i> 2015 , 23, A791.
$\text{YAG}:\text{Ce}^{3+}$	71%	<i>J. Soc. Inf. Display.</i> 2014 , 22, 419.

h-Bn = hexagonal boron nitride.

Table S5. Crystal Data and Structural Refinements for compound [TMPDA]₂Pb₃Br₁₀.

chemical formula	C ₁₄ H ₄₀ N ₄ Pb ₃ Br ₁₀
fw	1685.17
Space group	<i>P2₁/c</i>
<i>a</i> /Å	11.7112(10)
<i>b</i> /Å	15.6589(13)
<i>c</i> /Å	11.8912(10)
<i>β</i> /°	118.7447(10)
<i>V</i> (Å ³)	1911.9(3)
<i>Z</i>	2
<i>D</i> _{calcd} (g·cm ⁻³)	2.927
Temp (K)	296(2)
<i>μ</i> (mm ⁻¹)	23.637
<i>F</i> (000)	1496
Reflections collected	18253
Unique reflections	4433
Reflections (<i>I</i> >2σ(<i>I</i>))	2874
GOF on <i>F</i> ²	0.989
<i>R</i> ₁ , <i>wR</i> ₂ (<i>I</i> >2σ(<i>I</i>)) ^a	0.0623/0.1570
<i>R</i> ₁ , <i>wR</i> ₂ (alldata)	0.1010/0.1821

^a $R_1 = \sum ||F_o| - |F_c|| / \sum |F_o|$, $wR_2 = \{ \sum w[(F_o)^2 - (F_c)^2]^2 / \sum w[(F_o)^2]^2 \}^{1/2}$

Table S6. Selected bond lengths (Å) and bond angles (°) for compound [TMPDA]₂Pb₃Br₁₀.

Pb(1)-Br(3)	2.8205(14)	Br(2)-Pb(1)-Br(5)#1	91.58(4)
Pb(1)-Br(1)	3.0018(17)	Br(5)-Pb(1)-Br(5)#1	90.01(4)
Pb(1)-Br(2)	3.0044(15)	Br(2)#2-Pb(2)-Br(2)	180
Pb(1)-Br(5)	3.0465(14)	Br(2)#2-Pb(2)-Br(1)#2	83.91(4)
Pb(1)-Br(5)#1	3.0706(16)	Br(2)-Pb(2)-Br(1)#2	96.09(4)
Pb(2)-Br(2)#2	3.0282(15)	Br(2)#2-Pb(2)-Br(1)	96.09(4)
Pb(2)-Br(2)	3.0282(15)	Br(2)-Pb(2)-Br(1)	83.91(4)
Pb(2)-Br(1)#2	3.0459(17)	Br(1)#2-Pb(2)-Br(1)	180.00(8)
Pb(2)-Br(1)	3.0459(17)	Br(2)#2-Pb(2)-Br(4)#2	83.73(4)
Pb(2)-Br(4)#2	3.0599(16)	Br(2)-Pb(2)-Br(4)#2	96.27(4)
Pb(2)-Br(4)	3.0599(16)	Br(1)#2-Pb(2)-Br(4)#2	83.28(4)
		Br(1)-Pb(2)-Br(4)#2	96.72(4)
Br(3)-Pb(1)-Br(1)	91.41(5)	Br(2)#2-Pb(2)-Br(4)	96.27(4)
Br(3)-Pb(1)-Br(2)	93.34(5)	Br(2)-Pb(2)-Br(4)	83.73(4)
Br(1)-Pb(1)-Br(2)	85.08(5)	Br(1)#2-Pb(2)-Br(4)	96.72(4)
Br(3)-Pb(1)-Br(5)	84.15(4)	Br(1)-Pb(2)-Br(4)	83.28(4)
Br(1)-Pb(1)-Br(5)	93.43(5)	Br(4)#2-Pb(2)-Br(4)	180
Br(2)-Pb(1)-Br(5)	177.06(5)	Pb(1)-Br(5)-Pb(1)#1	89.99(4)
Br(3)-Pb(1)-Br(5)#1	91.15(5)	Pb(1)-Br(2)-Pb(2)	83.11(4)
Br(1)-Pb(1)-Br(5)#1	175.90(5)	Pb(1)-Br(1)-Pb(2)	82.86(4)


Symmetry transformations used to generate equivalent atoms: #1 -x+1, -y+1, -z+2; #2 -x, -y+1, -z+1.


Table S7. Hydrogen bonds data for compound [TMPDA]₂Pb₃Br₁₀.

D-H...A	d(D-H)	d(H...A)	d(D...A)	<(DHA)
N(1)-H(1)···Br(4)	0.98	2.37	3.3514(3)	174
N(2)-H(2)···Br(3)	0.98	2.46	3.3692(3)	155
C(1)-H(1A)···Br(3)	0.96	2.86	3.6594(3)	141
C(3)-H(3A)···Br(5)	0.97	2.84	3.6188(3)	138
C(4)-H(4B)···Br(2)	0.96	2.9	3.6403(3)	134
C(6)-H(6B)···Br(5)	0.97	2.84	3.7261(3)	152

References

- 1 C. K. Zhou, H. R. Lin, J. Neu, Y. Zhou, M. Chaaban, S. J. Lee, M. Worku, B. H. Chen, R. Clark, W. H. Cheng, J. J. Guan, P. Djurovich, D. Z. Zhang, X. J. Lv, J. Bullock, C. Pak, M. Shatruk, M. H. Du, T. Siegrist and B. W. Ma, *ACS Energy Lett.* **2019**, *4*, 1579-1583.
- 2 M. Z. Li, Y. W. Li, M. S. Molokeev, J. Zhao, G. R. Na, L. J. Zhang and Z. G. Xia, *Adv. Opt. Mater.* **2020**, 2000418.
- 3 M. Z. Li, J. Zhou, G. J. Zhou, M. S. Molokeev, J. Zhao, V. Morad, M. V. Kovalenko and Z. G. Xia, *Angew. Chem. Int. Ed.* **2019**, *58*, 18670-18675.
- 4 J. Zhou, M. Z. Li, L. X. Ning, R. L. Zhang, M. S. Molokeev, J. Zhao, S. Q. Yang, K. L. Han and Z. G. Xia, *J. Phys. Chem. Lett.* **2019**, *10*, 1337-1341.
- 5 Q. Li, Z. W. Chen, M. Z. Li, B. Xu, J. Han, Z. S. Luo, L. Tan, Z. G. Xia and Z. W. Quan, *Angew. Chem. Int. Ed.* **2020**, *60*, 2583-2587.
- 6 L. L. Mao, P. J. Guo, S. X. Wang, A. K. Cheetham and R. Seshadri, *J. Am. Chem. Soc.* **2020**, *142*, 13582-13589.
- 7 L. J. Xu, X. S. Lin, Q. Q. He, M. Worku and B. W. Ma, *Nat. Commun.* **2020**, *11*, 4329.
- 8 L. K. Gong, Q. Q. Hu, F. Q. Huang, Z. Z. Zhang, N. N. Shen, B. Hu, Y. Song, Z. P. Wang, K. Z. Du and X. Y. Huang, *Chem. Commun.* **2019**, *55*, 7303-7306.
- 9 M. Z. Li, J. Zhou, G. J. Zhou, M. S. Molokeev, J. Zhao, V. Morad, M. V. Kovalenko and Z. G. Xia, *Angew. Chem. Int. Ed.* **2019**, *58*, 18670-18675.

- 
- 10 Y. L. Wei, J. Jing, C. Shi, H. Y. Ye, Z. X. Wang and Y. Zhang, *Inorg. Chem. Front.* **2018**, *5*, 2615-2619.
- 11 V. Morad, I. Cherniukh, L. Pötttschacher, Y. Shynkarenko, S. Yakunin and M. V. Kovalenko, *Chem. Mater.* **2019**, *31*, 10161–10169.
- 12 Y. D. Deng, X. H. Dong, M. Yang, H. M. Zeng, G. H. Zou and Z. E. Lin, *Dalton Trans.* **2019**, *48*, 17451-17455.
- 13 B. B. Su, M. S. Molokeevbcd and Z. G. Xia, *J. Mater. Chem. C*, **2019**, *7*, 11220-11226.
- 14 L. J. Xu, A. Plaviak, X. S. Lin, M. Worku, Q. Q. He, M. Chaaban, B. J. Kim and B. W. Ma, *Angew. Chem. Int. Ed.* **2020**, *51*, 23067-23071.
- 15 M. E. Sun, Y. Li, X. Y. Dong and S. Q. Zang, *Chem. Sci.* **2019**, *10*, 3836-3839.
- 16 T. Ahmed, S. Seth and A. Samanta, *Chem. Mater.* **2018**, *30*, 3633–3637.
- 17 T. Zhao, H. B. Liu, M. E. Ziffer, A. Rajagopal, L. J. Zuo, D. S. Ginger, X. S. Li and A. K. Y. Jen, *ACS Energy Lett.* **2018**, *3*, 1662-1669.
- 18 D. J. Yu, F. Cao, Y. J. Gao, Y. H. Xiong and H. B. Zeng, *Adv. Funct. Mater.* **2018**, 1800248.
- 19 S. Kumar, J. Jagielski, N. Kallikounis, Y. H. Kim, C. Wolf, F. Jenny, T. Tian, C. J. Hofer, Y. C. Chiu, W. J. Stark, T. W. Lee and C. J. Shih, *Nano. Lett.* **2017**, *17*, 5277-5284.
- 20 P. S. Luna, J. N. Alapont, M. Sessolo, F. Palazon and H. J. Bolink, *Chem. Mater.* **2019**, *31*, 10205-10210.
- 21 S. X. Li, L. Wang, D. M. Tang, Y. J. Cho, X. J. Liu, X. T. Zhou, L. Lu, L. Zhang, T. Takeda, N. Hirosaki and R. J. Xie, *Chem. Mater.* **2017**, *30*, 494-505.
- 22 E. H. Song, Y. Y. Zhou, Y. Wei, X. X. Han, Z. R. Tao, R. L. Qiu, Z. G. Xia and Q. Y. Zhang, *J. Mater. Chem. C*, **2019**, *7*, 8192-8198.
- 23 Y. L. Zhu, Y. J. Liang, S. Q. Liu, H. R. Li and J. H. Chen, *Adv. Opt. Mater.* **2019**, 1801419.
- 24 P. Strobel, S. Schmiechen, M. Siegert, A. Tücks, P. J. Schmidt and W. Schnick, *Chem. Mater.* **2015**, *27*, 6109.
- 25 T. Takeda, N. Hirosaki, S. Funahshi and R. J. Xie, *Chem. Mater.* **2015**, *27*, 5892.
- 26 M. Zhao, H. X. Liao, L. X. Ning, Q. Y. Zhang, Q. L. Liu and Z. G. Xia, *Adv. Mater.* **2018**, *30*, 1802489.



27 J. S. Lee, S. Unithrattil, S. Kim, I. J. Lee, H. Lee and W. B. Im, *Opt. Lett.* **2013**, 38, 3298.

28 G. M. Sheldrick, *Acta Crystallogr. Sect. C* **2015**, 71, 3.

29 M. D. Segall, P. J. D. Lindan, M. J. Probert, C. J. Pickard, P. J. Hasnip, S. J. Clark, M. C. Payne, *J. Phys.: Condens. Matter.* **2002**, 14, 2717-2744.